Lck bound to coreceptor is less active than free Lck

Qianru Wei[a], Joanna Brzostek[a], Shvetha Sankaran[a,b], Javier Casas[c,d], Lois Shi-Qi Hew[a], Jiawei Yap[a], Xiang Zhao[a,1], Lukasz Wojciech[a], and Nicholas R. J. Gascoigne[a,b,2]

[a]Department of Microbiology and Immunology, Yong Loo Lin School of Medicine, National University of Singapore, Singapore, 117545; [b]Immunology Programme, Life Sciences Institute, National University of Singapore, Singapore, 117456; [c]Department of Biochemistry, Molecular Biology and Physiology, Universidad de Valladolid, Valladolid, Spain, 47005; and [d]Instituto de Biología y Genética Molecular, Consejo Superior de Investigaciones Científicas, Universidad de Valladolid, Valladolid, Spain, 47003

Edited by Jonathan Sprent, Garvan Institute of Medical Research, Darlinghurst, NSW, Australia, and approved May 27, 2020 (received for review August 2, 2019)

Src family kinase Lck plays critical roles during T cell development and activation, as it phosphorylates the TCR/CD3 complex to initiate TCR signaling. Lck is present either in coreceptor-bound or coreceptor-unbound (free) forms, and we here present evidence that the two pools of Lck have different molecular properties. We discovered that the free Lck fraction exhibited higher mobility than CD8α-bound Lck in OT-I T hybridoma cells. The free Lck pool showed more activating Y394 phosphorylation than the coreceptor-bound Lck pool. Consistent with this, free Lck also had higher kinase activity, and free Lck mediated higher T cell activation as compared to coreceptor-bound Lck. Furthermore, the coreceptor-Lck coupling was independent of TCR activation. These findings give insights into the initiation of TCR signaling, suggesting that changes in coreceptor-Lck coupling constitute a mechanism for regulation of T cell sensitivity.

Lck | coreceptor | T cell signaling | T cell receptor | T cell development

T cell activation commences with the recognition by T cell receptors (TCR) on the surface of a T cell membrane of the antigenic peptides presented by major histocompatibility complex (MHC) proteins on the surface of antigen-presenting cells (APC). At the initiation of signal transduction, the Src-family kinases (SFK) Lck and, to a lesser extent, Fyn, are recruited to phosphorylate the immunoreceptor tyrosine-based activation motifs (ITAMs) in the CD3 chains of the TCR complex (1–3). The phosphorylated ITAMs then allow binding of the Zeta chain-associated protein kinase 70 (Zap70) (1, 4). CD4 and CD8 coreceptors are recruited to the immunological synapse (IS) and bind to MHC-II and MHC-I, respectively (5). Lck can be bound to CD4 or CD8 coreceptors or unbound (free). The ITAM-bound Zap70 kinase molecules are then phosphorylated by Lck and transduce the signal to downstream molecules (2). Some evidence suggests that signal initiation caused by TCR–pMHC interactions starts with a SFK-dependent signal that does not require coreceptor-pMHC binding and that this is followed by a coreceptor-dependent phase of enhancing the TCR–pMHC complex formation (1, 6).

Like other SFKs, Lck contains a unique N-terminal sequence followed by SH3, SH2, and tyrosine kinase domains, ending with a C-terminal negative regulatory domain (2, 7). Lck exists in the cytosol and anchors to the inner leaflet of the plasma membrane (PM) through myristoylation and palmitoylation (2), or it binds to coreceptors through a zinc clasp structure formed by its conserved CxxC motif (C20 and C23) and a CxCP motif in CD4 (C420 and C422) or CD8α (C194 and C196) (numbering as in mouse proteins) (7, 8). The CD4 cytoplasmic tail can bind to significantly more Lck than CD8α's cytoplasmic tail (9). Experimentally increasing CD8-Lck coupling enhances proximal signaling and cellular responses, as the frequency of coreceptor-Lck coupling determines the kinetics of Lck delivery to the TCR (9). Both coreceptor-bound and coreceptor-unbound Lck can initiate CD3 phosphorylation upon TCR activation, where the free Lck can be recruited to the TCR complex and can trigger TCR signaling earlier than the coreceptor-bound Lck (10). However, it is currently unknown how coreceptor-Lck coupling regulates the kinetics of Lck delivery to the TCR during T cell development or after T cell activation.

Lck activity is tightly regulated by the phosphorylation and dephosphorylation of the activating tyrosine 394 (Y394) and the inhibitory Y505 (11). The Y505 of Lck can be phosphorylated by C-terminal Src kinase (Csk), resulting in a closed conformation with inhibited kinase activity (11). In contrast, the transmembrane tyrosine phosphatase CD45 dephosphorylates SFKs primarily on their C-terminal negative regulatory sites through the association between CD45 and Y192 of Lck (12), allowing the kinases to form an open conformation (11). The activating Y394 of Lck can be autophosphorylated by Lck, resulting in a stabilized open structure and enhanced kinase activity and substrate binding (11). Dephosphorylation of the Y394 site is regulated by several phosphatases, including CD45, SH2 domain-containing phosphatase 1 (SHP-1), PEST-domain enriched tyrosine phosphatase (PEP), and protein tyrosine phosphatase-PEST (13–16). The Y394 and Y505 double unphosphorylated Lck has a basal amount of kinase activity (11), and the Y394 and Y505 double phosphorylated Lck has similar activity to the Y394 single-phosphorylated Lck (17). Activated Lck can be detected in mouse T cells and thymocytes prior to TCR stimulation in vitro and in vivo, and the percentage of activated Lck (about 50%) remained unchanged after stimulation (13, 17). Among the total Lck, the Y394 and Y505 double-unphosphorylated, single-phosphorylated, and

Significance

Lck is critical for T cell development and activation, as it is the first kinase transducing TCR signaling. Lck can be bound or not bound (free) to the coreceptors (CD4 and CD8) in thymocytes and T cells. After comparing molecular properties of free and coreceptor-bound Lck, free Lck presents higher mobility and activity compared to the coreceptor-bound Lck. The coreceptor-Lck coupling is found to be independent of TCR activation. This information is valuable for better understanding the initiation of TCR signaling and the regulation of T cell sensitivity.

Author contributions: Q.W., J.B., J.C., X.Z., and N.R.J.G. designed research; Q.W., J.B., S.S., and L.S.-Q.H. performed research; J.Y. and L.W. contributed new reagents/analytic tools; Q.W., J.B., S.S., J.C., and N.R.J.G. analyzed data; and Q.W., J.B., and N.R.J.G. wrote the paper.

The authors declare no competing interest.

This article is a PNAS Direct Submission.

Data deposition: Sequence data have been deposited in the National Center for Biotechnology Information GenBank database, https://www.ncbi.nlm.nih.gov/genbank (accession nos. MT591673–MT591676).

[1]Present address: Department of Molecular and Cellular Physiology, Stanford University, Stanford, CA 94305.

[2]To whom correspondence may be addressed. Email: micnrjg@nus.edu.sg.

This article contains supporting information online at https://www.pnas.org/lookup/suppl/doi:10.1073/pnas.1913334117/-/DCSupplemental.

double-phosphorylated fractions each represented ~25% in Jurkat cells (17).

As the first kinase transducing the TCR signaling after TCR and pMHC recognition, Lck has been extensively studied. However, previous studies examined the total Lck pool, and very little is known about how coreceptor binding alters Lck's molecular properties. As CAR-T cells do not use canonical pMHC recognition involving coreceptors, and are likely to rely on free Lck, a better understanding of the molecular properties of free and bound Lck pools is important for designing better immunotherapy strategies. We sought to compare the molecular properties of CD8-bound and free Lck fractions in primary mouse T cells and OT-I T cell hybridoma. Our data show that free Lck has higher mobility, more Y394 phosphorylation, and higher kinase activity than the coreceptor-bound Lck.

Results

Free Lck Pool Has Higher Mobility than Coreceptor-Bound Lck Pool. Previous research showed that free Lck is recruited to the IS before CD8-bound Lck after TCR activation (10). To explore the mechanism of this finding, we hypothesized that the free and coreceptor-bound Lck molecules in T cells have different mobility. We established a Lck knockout OT-I TCR CD8αβ$^+$ hybridoma system (OT-I.CD8αβ$^+$.endoLck$^{-/-}$) using CRISPR/Cas9 (18) (*SI Appendix*, Fig. S1) and then transduced either free Lck(C20.23A)-mCherry or covalently linked CD8α-Lck-mCherry (*SI Appendix*, Fig. S3*A*). We performed fluorescent recovery after photobleaching (FRAP) imaging to analyze the kinetics of Lck diffusion on the cell membrane. Cells were loaded onto lipid bilayers containing mouse ICAM-1 to facilitate cell attachment and incubated at 37 °C for 30 min before imaging. This allows the cells to settle onto the bilayers through the association between ICAM-1 and the adhesion molecule LFA-1 on the hybridoma cells. This process does not trigger TCR activation. Therefore, the basal-level mobility of these Lck molecules can be measured. Both free and coreceptor-bound Lck were localized at the cell membrane (Fig. 1 *A*–*C*), so we analyzed the membrane area adhering to the lipid bilayers using confocal microscopy. The difference in mobility of free and CD8-bound Lck were clearly shown in the fluorescence recovery curves (Fig. 1 *B* and *C*). Although the difference in the percentages of the mobile fraction of the free and coreceptor-bound Lck in OT-I hybridoma cells was small (~80% and ~70%, respectively), the time from the photobleaching until fluorescence half recovery (half time of recovery) of the two Lck pools exhibited a significant difference (Fig. 1*E*). The half time of free Lck recovery (~2.9 s) was around half that of CD8α-Lck (~5.5 s), indicating that free Lck has approximately twice the mobility of coreceptor-bound Lck in these cells (Fig. 1*E*). Lck(C20.23A)-mCherry (free Lck) or CD8α-Lck-mCherry expressed in 293T cells also showed similar results (*SI Appendix*, Fig. S2). Together, these results demonstrated that the free Lck fraction has a higher basal level of mobility than the CD8α-bound Lck fraction in OT-I hybridoma and 293T cells. The difference in mobility may explain why free Lck is recruited faster to the IS than CD8-bound Lck after T cell activation, as we previously observed (10). The mobility difference was not T cell restricted, hence this mobility difference may relate to the molecular weight of free and CD8α-bound Lck, the size of the extracellular domain, and the presence/absence of a transmembrane domain; free Lck is smaller than coreceptor-bound Lck in molecular weight and is only bound to the inner leaflet of the plasma membrane, if at all, whereas the location and mobility of the coreceptor-bound Lck is limited by the much larger transmembrane coreceptors with big extracellular domains.

Free Lck Pool Contains More pY394 than Coreceptor-Bound Pool in T Hybridoma Cells. We have previously demonstrated that free Lck is recruited to the TCR complex before the coreceptor-bound Lck (10). This may be due to the differential activity of free and coreceptor-bound Lck. We tested the phosphorylation states of free and coreceptor-bound Lck in hybridomas expressing both Lck(C20.23A)-mCherry and CD8α-Lck-Cerulean (the hybridoma cells referred to as OT-I.8αLckC.LckC2023A.R) (*SI Appendix*, Fig. S4*B*). To verify that the constructs were truly coreceptor-bound and coreceptor-unbound, CD8α was immunoprecipitated from cell lysates. As expected, the Lck(C20.23A)-mCherry protein was not coprecipitated with CD8, but the Lck expressed in the CD8α-Lck-Cerulean format was constitutively bound to CD8α (*SI Appendix*, Fig. S3*B*). The specificity of the antibodies recognizing differential Lck phosphorylation is critical for the quantification of the different activation states of Lck. We used Y394F and Y505F mutated Lck proteins to confirm specificity of the antibodies recognizing pY394 Lck and pY505 Lck (*SI Appendix*, Fig. S3 *C*–*E*). To test the specificity of anti-Y394–nonphosphorylated Lck antibody, hybridomas expressing WT Lck-mCherry or Lck(Y394F)-mCherry proteins were treated with pervanadate (PV, inhibitor of tyrosine phosphatases) or PP2 (SFK inhibitor that reduces Lck autophosphorylation at Y394) to obtain increased or decreased phosphorylation of Lck, respectively (*SI Appendix*, Fig. S3*E*). The Y394-nonphosphorylated Lck signal was reduced after PV treatment and increased after PP2 treatment in WT Lck, but the signal remained unchanged in the Y394F Lck after PV or PP2 treatments (*SI Appendix*, Fig. S3*E*). Therefore, anti-Y394–nonphosphorylated Lck antibody can specifically recognize the Lck Y394 unphosphorylated proteins. Lck can transautophosphorylate its Y394 site even after cell lysis (19), which may result in higher activity detected by Western blotting (WB) or immunoprecipitation (IP). To maintain Lck phosphorylation after cell lysis, SFK inhibitor PP2 (20 μM) together with a protease-phosphatase inhibitor mixture (*Materials and Methods*) were supplemented into the lysis buffer during cell lysis and IP incubation (19) (*SI Appendix*, Fig. S4*A*). Using these validated antibodies and an optimized cell lysis method, Lck active phosphorylation status can be reported by the intensity ratio of pY394-Lck (active Lck)/Y394-nonphospho-Lck (inactive Lck) detected by WB, as treatment with pervanadate (phosphatase inhibitor) or PP2 (SFK inhibitor) results in a higher and a lower ratio, respectively (Fig. 2*A*).

OT-I.8αLckC.LckC2023A.R cells, coexpressing both free and constitutively coreceptor-bound Lck molecules, were lysed and analyzed using the approach outlined above. The intensity ratio of pY394 versus Y394-nonphospho Lck, as well as pY505-Lck versus total Lck, were quantified on the same immunoblots using LI-COR fluorescent imaging system (*SI Appendix*, Fig. S4*B*). The free Lck(C20.23A)-mCherry and bound CD8α-Lck-Cerulean appeared at distinct locations on the blot due to the higher molecular weight of the CD8α-bound Lck fusion (*SI Appendix*, Fig. S4*B*). The ratio of active pY394 Lck to inactive Y394-nonphospho Lck in the free Lck pool was significantly greater than in the coreceptor-bound Lck pool, while the pY505/total Lck ratio was significantly higher in the coreceptor-bound Lck pool (*SI Appendix*, Fig. S4 *B* and *C*). This result suggests that there is a difference in Lck activation status between free and CD8-bound Lck fractions in the hybridoma cells, and that free Lck is more active than CD8-bound Lck. Next, we tested if this difference in Lck activation status between free and CD8-bound Lck fractions changed after TCR activation. The cells contain a small amount of endogenous Lck (*SI Appendix*, Fig. S1 *C* and *D*) may affect the phosphorylation status of the overexpressed Lck mutants. Hence, the endogenous Lck-deficient OT-I.CD8αβ$^+$.endoLck$^{-/-}$0.8αLckC.LckC2023A.R cells were used for the following experiment. OT-I TCR binds to ovalbumin (OVA) peptide 257–264 (SIINFEKL) presented by H2K^b with high affinity, whereas Q4R7, one of the OVA altered peptide ligands (APLs), has moderate affinity to OT-I TCR (9, 20, 21). The OT-I hybridomas were stimulated with H2-K^b-OVA, H2-K^b-Q4R7,

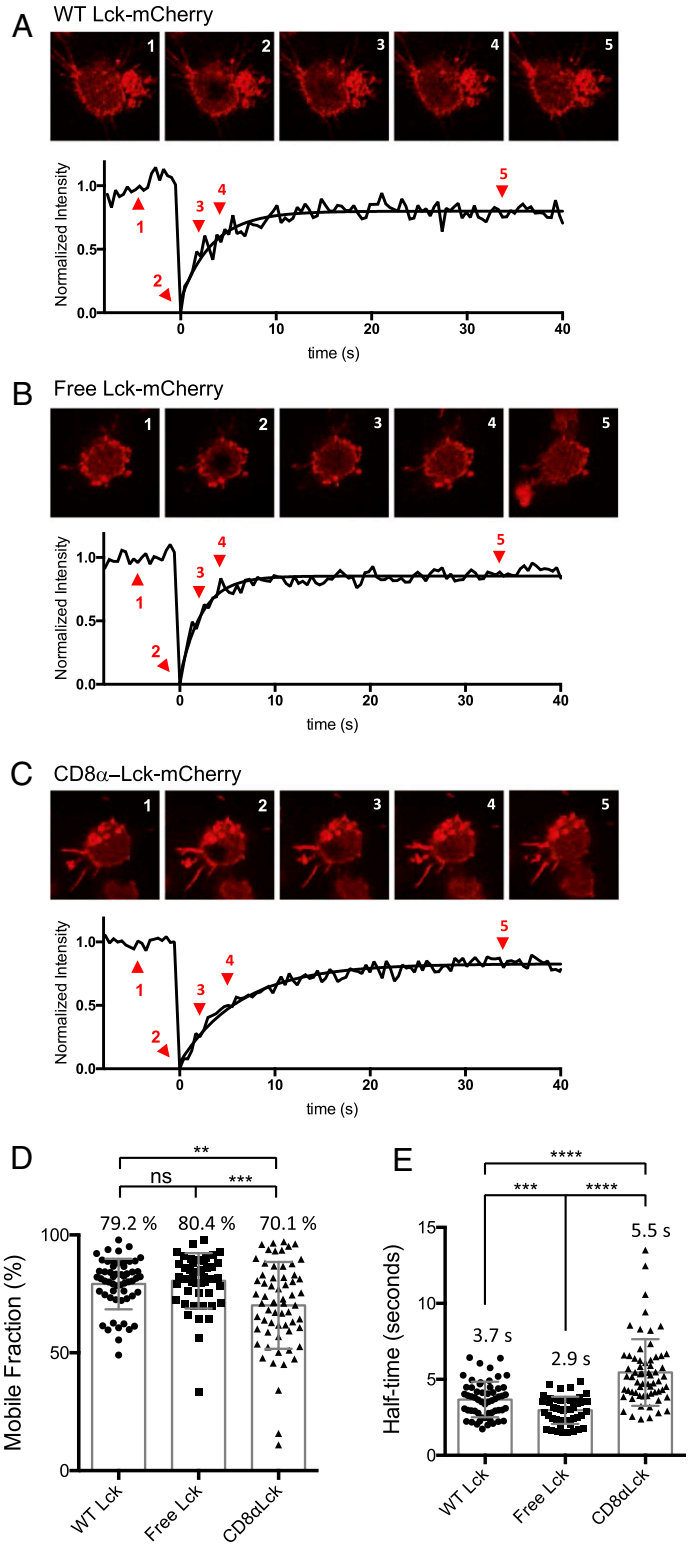

Fig. 1. Mobility of free Lck and CD8α-Lck in OT-I hybridomas. OT-I.CD8αβ^{+}.endoLck$^{-/-}$ hybridoma cells were transduced with WT Lck, C20.23A mutant Lck (free Lck), or CD8α-bound Lck that was fused with mCherry. The lipid bilayers contained mouse ICAM-1 and Streptavidin-Alexa Fluor 488. The hybridoma cells were loaded onto the lipid bilayers and incubated at 37 °C for at least 30 min prior to the FRAP imaging experiment. (*A*–*C*) The fluorescent intensity recovery curves of WT (*A*), free (*B*), and CD8α-bound Lck (*C*). The normalized intensity indicates the average intensity of the photobleached area normalized to prebleach, the fluorescence loss, and the first photobleach after background subtraction. The normalized intensity was fitted using one-phase association by Prism software. The cell images at prebleach (*1*, $x = -4.5$ s), bleach (*2*, $x = 0$ s), incomplete recovery (*3*, $x = 2.2$ s; *4*, $x = 4.4$ s) and complete recovery (*5*, $x = 34.4$ s) are presented. The mobile fraction (*D*) and half-time (*E*) were analyzed by Prism software. The significance was analyzed by Student's *t* test, ns, not significant; *$P < 0.05$; **$P < 0.01$; ***$P < 0.001$; and ****$P < 0.0001$. Mean ± SEM of WT Lck, $n = 56$; free Lck, $n = 48$; and CD8α-Lck, $n = 63$ are shown. The figure is representative of three independent experiments.

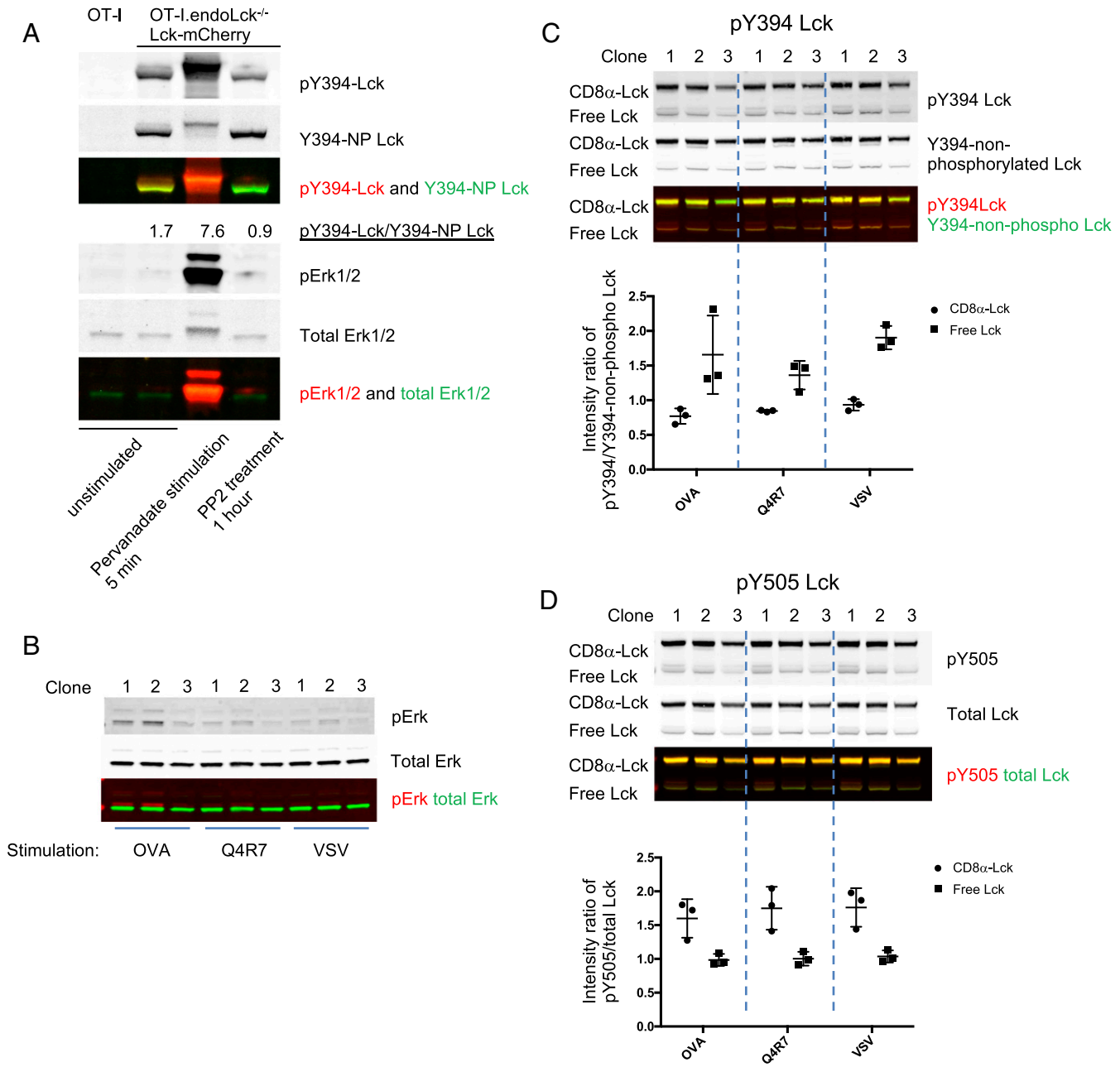

Fig. 2. Higher Y394 phosphorylation in free Lck than CD8-bound Lck fraction in T hybridoma cells. (*A*) OT-I endoLck$^{-/-}$ CD8αβ-expressing hybridoma cells (OT-I.CD8αβ^{+}.endoLck$^{-/-}$) overexpressing Lck-mCherry were unstimulated, stimulated with Pervanadate (PV) for 5 min, or treated with PP2 inhibitor for 1 h before lysis. Signal intensity ratios of pY394/Y394-NP Lck were calculated. (*B–D*) OT-I.CD8αβ^{+}.endoLck$^{-/-}$ hybridoma cells transduced with both CD8α-Lck-Cerulean and Lck(C20.23A)-mCherry were sorted as single clones (OT-I.CD8αβ^{+}.endoLck$^{-/-}$0.8αLckC.LckC2023A.R). The cell clones were stimulated by H2-K^{b}-OVA/Q4R7/VSV tetramers for 5 min before lysis. The Erk phosphorylation (*B*), pY394/Y394-NP Lck (*C*), or pY505/total Lck (*D*) levels of each cell lysis were detected by WB. The intensity ratio of pY394/Y394-NP Lck or pY505/total Lck of free and coreceptor-bound Lck were summarized. Mean ± SEM is shown. The figure is representative of two independent experiments.

or H2-K^{b}-VSV (negative control) tetramers for 5 min. As shown in Fig. 2 *B–D*, the pY394/Y394-nonphospho Lck ratio was higher, and the pY505/total Lck ratio was lower, in the free Lck compared to CD8-bound Lck, thus confirming our earlier observations. However, the phosphorylation status of free and CD8-bound Lck did not change in response to changes to the strength of TCR activation (Fig. 3 *C* and *D*). These results indicate that free Lck has more phosphorylation at the activating site Y394 than does coreceptor-bound Lck, regardless of the strength of TCR activation.

Free Lck Pool Has More Y394 Phosphorylation than Coreceptor-Bound Pool in Ex Vivo T Cells. To further investigate the phosphorylation states of free and coreceptor-bound Lck in mouse thymocytes and primary T cells, a sequential IP method was applied to separate the free and coreceptor-bound Lck pools (Fig. 3*A*). CD4^{+}CD8^{+} double positive (DP) thymocytes and naïve CD4^{+} T cells were sorted from WT B6 mice, and naïve CD8^{+} T cells were sorted from OT-I transgenic mouse lymphocytes. The cells were then lysed and immunoprecipitated with anti-CD4 and/or CD8α antibodies. Part of the whole cell lysate (WCL) and the

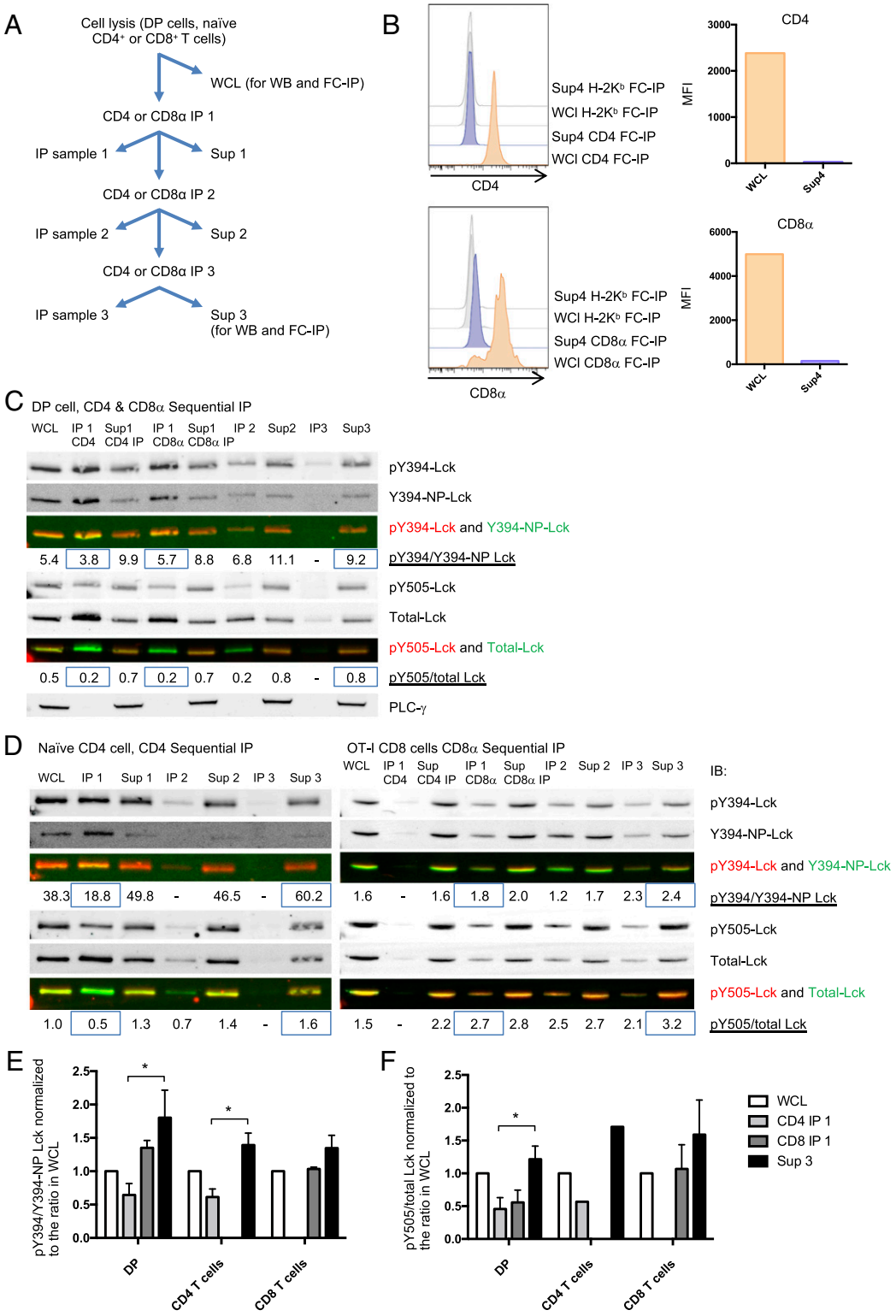

Fig. 3. Higher Y394 phosphorylation in free Lck than CD8-bound Lck fraction in mouse primary DP and peripheral T cells. (*A*) Illustration of the sequential IP method. (*B*) DP cell WCL and supernatant 3 (40 μL each) were harvested for FC-IP analysis. CD4, CD8α, or H2K^b coated beads were added into the WCL or supernatant 3 and incubated overnight. Beads were washed and stained with anti-CD4-PE or anti-CD8β-PE antibodies. Histograms of the CD4, CD8β, and background (H2K^b beads) staining (*B*, *Left*) and the MFI subtracted backgrounds (*B*, *Right*) are presented. (*C*) CD4 and CD8α sequential IP was performed on DP thymocytes. (*D*, *Left*) CD4 sequential IP was performed on naïve CD4$^+$ T cells sorted from WT mouse lymphocytes. (*D*, *Right*) CD8α IP was performed on naïve CD8 T$^+$ cells sorted from OT-I transgenic mice. The pY394-Lck, Y394-nonphospho Lck, pY505-Lck, and total Lck were detected by WB. pY394 Lck was detected by anti-pY416-Src antibody. The intensity ratio pY394/Y394-nonphosphorylated Lck and Y505/total Lck were quantified and indicated on the figure. *C* is representative of three independent experiments; *D* is representative of two independent experiments. (*E* and *F*) The pY394/Y394-NP-Lck and Y505/total Lck intensity ratios on each WB gel were normalized to WCL samples. *E* and *F* represent the summary of three repeats of DP cells and two repeats of naïve CD4 and naïve CD8 cells. The significance was analyzed by paired *t* test, $*P < 0.05$. Mean ± SEM is shown.

supernatant 3 were kept for flow cytometry IP (FC-IP) analysis. As shown in Fig. 3*B*, the majority of the CD4 or CD8 coreceptors were depleted from the supernatant after three rounds of IP. After this coreceptor depletion, the phosphorylation states of coreceptor-bound (IP fraction from the first round of IP) and free (supernatant fraction after three rounds of IP) Lck molecules were quantified by WB (Fig. 3 *C* and *D*). Low yet detectable free Lck signals were found in the supernatant from DP cells, naïve CD4 T cells, and naïve CD8 T cells (Fig. 3 *C* and *D*). After normalizing the ratio of pY394 to Y394-nonphospho-Lck intensity to the WCL sample in each experiment, we observed that this ratio was higher for the free Lck pool compared to the coreceptor-bound Lck pool in DP, naïve CD4, and naïve CD8 T cells (Fig. 3 *C*–*F*). Similarly, the pY505/total Lck ratio was also higher in the free Lck pool compared to the coreceptor-bound pool (Fig. 3 *C*–*F*). This indicates that in the free Lck pool of mouse primary cells, less Lck was in the "primed" state (Y394 and Y505 both not phosphorylated) compared to coreceptor-bound Lck. Although the Y505 phosphorylation may result in closed conformation of Lck, the Y394 and Y505 double-phosphorylated Lck still remains open and has kinase activity (17). Overall, these results from primary T cells, together with the data obtained using OT-I hybridomas, strongly suggest that free and coreceptor-bound Lck pools differ in their phosphorylation status, and that the free Lck pool was more active than the coreceptor-bound Lck pool in primary mouse DP and peripheral T cells.

We then investigated coreceptor-Lck coupling upon activation of peripheral T cells by FC-IP, which allows quantitative analysis of the Lck-coupled coreceptor (22–24). For the FC-IP, CD4 or CD8β coreceptors were immunoprecipitated by latex beads coated with capture antibody, then CD4, CD8α, and Lck were detected using PE-conjugated detection antibodies. The capture and detection antibodies for CD4 and CD8αβ do not block the binding of each other's epitope on CD4 or CD8 (*SI Appendix*, Fig. S5). The mean fluorescence intensity (MFI) of each marker on the beads was analyzed by flow cytometry, and MFI values were converted into PE molecules per bead, based on values from standards generated by BD Quantibrite beads (*SI Appendix*, Fig. S6 *A* and *B*). Naïve $CD4^+$ and $CD8^+$ T cells sorted from WT mice were stimulated either with plate-bound anti-CD3ε and anti-CD28 antibodies for 24 h, or not stimulated (*SI Appendix*, Fig. S6*C*). We confirmed that cells were stimulated using cell surface staining to detect cell surface expression of activation markers (*SI Appendix*, Fig. S6*C*). Cells were then lysed and analyzed by FC-IP. Approximately 34% of CD4 coreceptors were bound with Lck in naïve $CD4^+$ T cells, and ∼4.6% of CD8αβ coreceptors were bound with Lck in naïve $CD8^+$ T cells (*SI Appendix*, Fig. S6*D*), which agreed with a recent report (25). This significantly higher Lck coupling for CD4 coreceptors than CD8 coreceptors may be due to the higher binding affinity between Lck and CD4 compared to Lck and CD8 (9, 26). After stimulation by anti-CD3ε plus anti-CD28 antibodies for 24 h, the coreceptor-Lck coupling did not change significantly in either CD4 or CD8 T cells (*SI Appendix*, Fig. S6*D*). These data suggest that Lck-coreceptor coupling is independent of TCR activation.

Free Lck Has Higher Kinase Activity Compared to Coreceptor-Bound Lck. After observing the phosphorylation status difference of free and coreceptor-bound Lck, we then further investigated if this resulted in a difference in functional activity. WT Lck, free Lck, and CD8α-bound Lck were immunoprecipitated by anti-mCherry antibody from lysates of OT-I.CD8αβ$^+$.endoLck$^{-/-}$ cells expressing either the WT Lck-mCherry, free Lck(C20.23A)-mCherry, or bound CD8αLck-mCherry. Untransduced OT-I.CD8αβ$^+$.endoLck$^{-/-}$ cells were used as negative control. After incubating the immunoprecipitated Lck proteins with CD3ζ-GST protein in Lck kinase buffer for 20 min at 37 °C, a significantly higher Y142-ζ phosphorylation was observed in the free Lck sample, followed by WT Lck. The coreceptor-bound Lck showed the lowest activity compared to free Lck and WT Lck (Fig. 4 *A* and *B*). This result strongly suggests that the kinase activity of free Lck is higher than the CD8-bound Lck. However, the above system measures the kinase activity of Lck from cells expressing only one form of Lck. To investigate more physiological conditions, where T cells have both free and coreceptor-bound Lck, we tested the kinase activity of Lck using OT-I.CD8αβ$^+$.endoLck$^{-/-}$ cells coexpressing free Lck(C20.23A)-mCherry and bound CD8α-Lck-eGFP molecules. In agreement with data from cells expressing single Lck species only, free Lck induced higher CD3ζ phosphorylation than coreceptor-bound Lck (Fig. 4*C*).

Next, we tested if both free and coreceptor-bound Lck can be involved in TCR signaling. The OT-I.CD8αβ$^+$.endoLck$^{-/-}$ cells (negative control) and such cells expressing either WT Lck-mCherry, free Lck(C20.23A)-mCherry, or bound CD8α-Lck-mCherry were stimulated by plate-bound anti-CD3ε antibody for 24 h. Supernatants were harvested for IL-2 ELISA experiments. As shown in Fig. 4*D*, secretion of IL-2 was significantly higher by cells overexpressing free Lck than those expressing coreceptor-bound Lck, whereas similar IL-2 concentrations were observed in WT Lck and free Lck-expressing cells. With the same set of cells, we measured the phosphorylation of early TCR signaling molecules (Zap70 and LAT) after stimulating the cells with anti-CD3 antibody cross-linking. Phosphorylation of Zap70 and LAT was only observed in the hybridoma cells expressing Lck molecules, with no differences between phosphorylation mediated by Lck, free Lck, or bound CD8α-Lck) (Fig. 4*E*). Critically, all Lck species can mediate Erk phosphorylation after CD3 cross-linking (Fig. 4*E*). These data suggest that both free Lck and CD8-bound Lck can mediate TCR signaling such that IL-2 secretion and phosphorylation of TCR signaling molecules Zap70, LAT, and Erk can be observed.

Discussion

In this research, we have shown that the free Lck pool has higher mobility, Y394 phosphorylation, and kinase activity than the coreceptor-bound Lck pool. The higher mobility and kinase activity of free Lck can enable free Lck to be recruited at the TCR complex and to initiate TCR signaling before the coreceptors and coreceptor-bound Lck. However, this coupling is independent of TCR activation.

Lck can be anchored into the cell membrane through myristoylation at serine 2 and palmitoylation at cysteine 3 and cysteine 5 (2). Lck palmitoylation was found to be reversible, and Lck palmitoylation is required for full membrane anchoring, because a Lck mutant that cannot be palmitoylated was not located at the membrane (27). Lck was also found to have a high palmitoylation turnover rate in resting T cells (28). Single-molecule analysis revealed that Lck did not undergo directed movement toward the TCR cluster but instead underwent short-term simple Brownian diffusion during the initiation of TCR signaling (29). Through FRAP imaging experiments, we found that membrane-associated but coreceptor-unbound Lck had higher basal mobility than the coreceptor-bound Lck. This mobility difference may be one of the direct reasons why free Lck was recruited to the IS earlier than CD8α-Lck after T cell activation (10). As the mobility difference was observed in both T cells and a non-T cell line, it may relate to the molecular size or to the size of the extracellular domain and/or the presence/absence of a transmembrane domain. Free Lck is smaller in size compared to the coreceptor-bound Lck and is only bound to the inner leaflet of the plasma membrane, if at all, whereas the location and mobility of the coreceptor-bound Lck is limited by the much larger, transmembrane coreceptors anchored into the cell membrane through their transmembrane regions. Although free Lck has a higher basal level of mobility compared to the

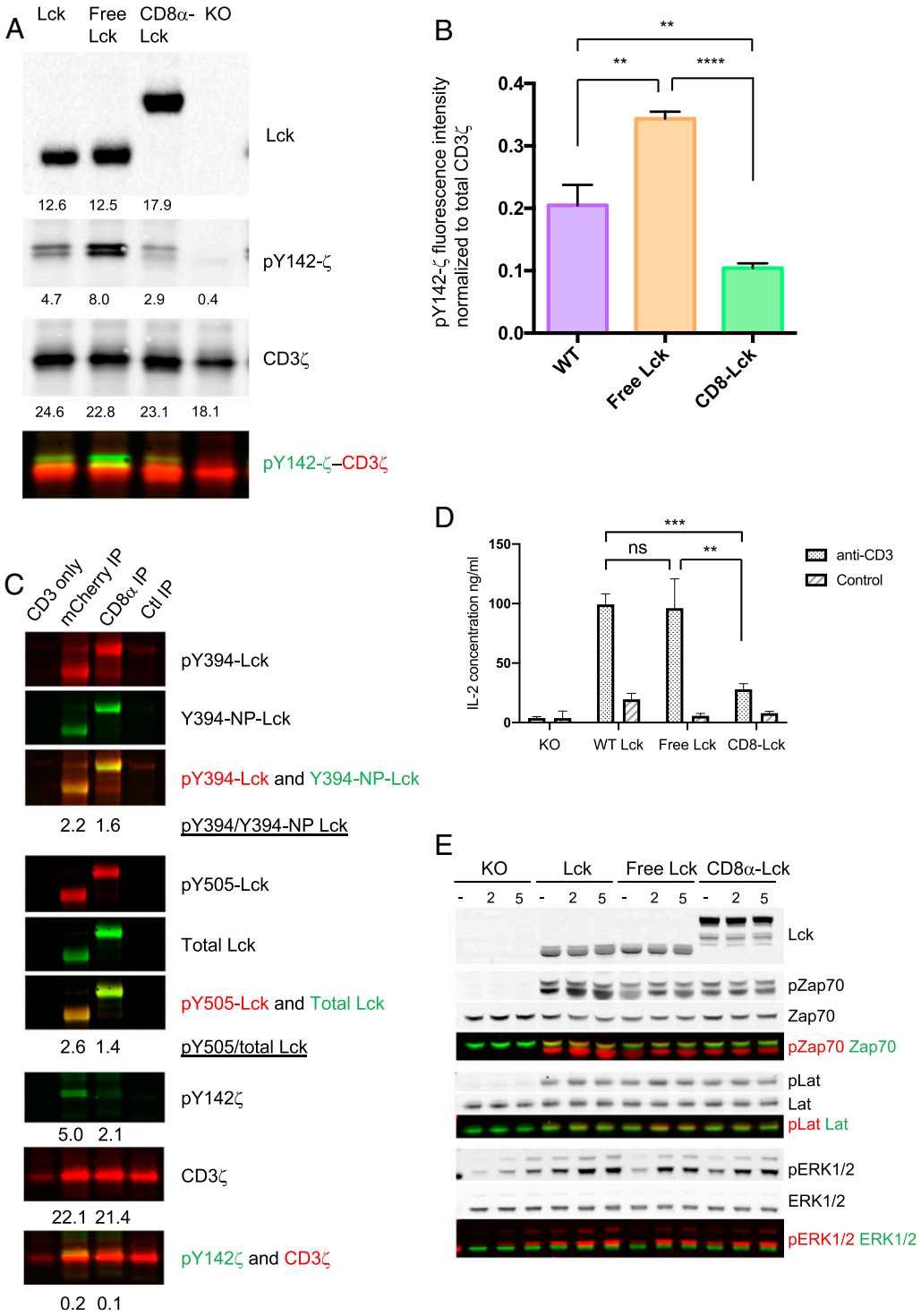

Fig. 4. Higher kinase activity in free Lck than CD8-bound Lck and both free and CD8-bound Lck can contribute in TCR signaling. (*A*) OT-I.CD8αβ^{+}.endoLck$^{-/-}$ hybridoma cells overexpressing WT Lck-mCherry, free Lck(C20.23A)-mCherry, or bound CD8α-Lck-mCherry were lysed, and Lck mutants were immunoprecipitated by anti-mCherry antibody. Lck knockout hybridoma cells were used as a negative control. The mCherry immunoprecipitations were assayed for kinase activity on CD3ζ-GST and immunoblotted for pY142-CD3ζ, total CD3ζ, and total Lck. (*B*) Kinase activity was analyzed by pY142-CD3ζ intensity subtracted for Lck knockout control and normalized for total CD3ζ intensity. (*C*) OT-I.CD8αβ^{+}.endoLck$^{-/-}$ hybridoma cells overexpressing both free Lck(C20.23A)-mCherry and bound CD8α-Lck-eGFP were lysed, and anti-mCherry, anti-CD8α, and control IP with an irrelevant antibody were performed. The immunoprecipitations were assayed for kinase activity on CD3ζ-GST and immunoblotted for pY142-CD3ζ, total CD3ζ, and total Lck. A representative experiment of two is shown. (*D*) OT-I.CD8αβ^{+}.endoLck$^{-/-}$ hybridoma cells expressing transfected Lck-mCherry, Lck(C20.23A)-mCherry, or CD8α-Lck-mCherry were stimulated by plate-bound anti-CD3ε antibody for 24 h. Cells cultured in PBS pretreated wells served as negative controls. Supernatants were harvested for mouse IL-2 ELISA. Statistical significance was analyzed by Student's *t* test: ns, not significant; $^{**}P < 0.01$; $^{***}P < 0.001$, Mean ± SEM is shown. A representative experiment of three is shown. (*E*) OT-I.CD8αβ^{+}.endoLck$^{-/-}$ hybridoma cells expressing transfected Lck-mCherry, Lck(C20.23A)-mCherry, or CD8α-Lck-mCherry were stimulated by cross-linking anti-CD3ε antibody for 2 min or 5 min. Stimulated or unstimulated cells were lysed and total Lck, phospho-Zap70, total Zap70, phospho-LAT, total LAT, phospho-Erk1/2, and total Erk were analyzed by WB. A representative experiment of three is shown.

coreceptor-bound Lck, it has been found that the membrane anchor was insufficient to modulate Lck movement toward TCR after TCR activation (30).

The initiation of TCR signaling after the interaction between TCR and pMHC includes a first SFK-mediated phase and a second stabilization phase when CD8-pMHC binding occurs (1, 6). Lck that is not bound to coreceptor and coreceptor-bound Lck were observed to colocalize with CD3ζ sequentially after TCR activation (10). By separating coreceptor-bound and free Lck pools, we have revealed that the free Lck pool contains a higher amount of active Lck (pY394-Lck) in OT-I hybridoma cells, primary mouse DP cells, and peripheral T cells. After TCR activation, free and CD8-bound Lck coexpressed in OT-I hybridoma cells showed the same phosphorylation status as in unstimulated cells. This result suggests that the differential activity of free and coreceptor-bound Lck is independent of TCR activation and drives the first SFK-mediated TCR activation stage. After TCR activation, the percentage of Lck-bound coreceptors also remained unchanged in both $CD4^+$ and $CD8^+$ T cells, indicating that Lck-coreceptor coupling is independent of TCR signaling.

During thymocyte development, coreceptor and Lck coupling is critical for TCR selection and lineage commitment (31). The interaction of Lck with CD4 and CD8 is essential to ensure that DP cells do not respond to non-MHC activation of TCR during thymic selection and is therefore critical for selecting the MHC-restricted αβTCR repertoire (31, 32). Recently, Lck and coreceptor coupling was shown to be higher in peripheral T cells compared to DP thymocytes (25). Although the percentage of Lck-bound coreceptors increases from DP to peripheral T cells, a fraction of Lck always exists that is unbound by the coreceptors. This low amount of free Lck in DP thymocytes is not sufficient to allow development of non-MHC–restricted T cells but may contribute to the modulation of TCR signaling during the thymic selection process. After positive and negative selection during the DP stage, thymocytes that have signaled in response to either MHC-I or MHC-II go through a $CD4^+CD8^{lo}$ stage, followed by entering the $CD4^-CD8^+$ (MHC-I lineage) or $CD4^+CD8^-$ (MHC-II lineage) single-positive stages (33, 34). The down-regulation of either coreceptor can release the previously bound Lck, and these Lck molecules may remain free or bind to other coreceptors, resulting in increased coreceptor-Lck coupling.

The cytoplasmic tail of CD8 has lower affinity to Lck than the CD4 coreceptor (9, 26), so Lck molecules are less frequently bound to CD8 than to CD4. In this study, CD8-bound Lck molecules were found to have a slightly higher Y394 phosphorylation than those bound to CD4 coreceptors in DP cells. Although CD4 coreceptors were found to have higher binding of Lck than CD8 (9, 26), we found that the Y394 phosphorylation of CD4-bound Lck is lower. Activated Lck has been reported to be released from CD4 (26), and this release could potentially lead to higher amounts of activated Lck in the free Lck fraction. CD8 T cells have faster and stronger responses to TCR activation than CD4 T cells, as they proliferate faster than CD4 T cells (35) and differentiate into memory T cells within a shorter time after virus infection (36). High amounts of free Lck in CD8 T cells and the higher activity of Lck that is bound to CD8 coreceptor may determine a quicker and stronger response. However, the higher amount of Lck sequestration in CD4 T cells may lead to a slower but more steady response of CD4 T cells after infection, supporting CD8 T cells and other immune cells by secreting cytokines. Recently, lymph node T cells of CD8.4 (CD8 coreceptor with a CD4 cytoplasmic tail) transgenic mice were found to have less self-reactivity compared to WT mice (25). This may due to the lower amount of free Lck that exists in the CD8.4 cells, as more Lck is bound by the CD8.4 in these T cells. Previously, decreased CD8-Lck coupling was observed after TCR stimulation of effector T cells (37). This conflicting result may be due to the different methods used, as the FC-IP method used in this research is more quantitative as compared to conventional IP.

Lck phosphorylation and dephosphorylation are tightly regulated by multiple kinases and phosphatases (2), and Lck Y394 can be autophosphorylated in trans (11). Therefore, the higher phosphorylation of Y394 in the free Lck pool may due to its higher autophosphorylation efficiency, resulting from its higher mobility. In the hybridoma cells expressing one form of Lck mutant, we observed a prephosphorylated population of Zap70 and LAT even before TCR stimulation. This may result from the recognition of endogenous peptide MHC in this experimental system, or to dysregulation of phosphatases in these cells. To further investigate the physiological conditions, transgenic mice with only free or coreceptor bound Lck could be used.

Lck has been a focus in CAR-T immunotherapy strategies (38–43). Combining Lck with CD3ζ chain in a single-chain CAR enhanced IL-2 production after CAR ligation compared to CD3ζ-CAR, and the amount of IL-2 production was similar to cells expressing CD28-incorporating CAR (38). CAR-T cell function can also be blocked by the tyrosine kinase inhibitor dasatinib, which interferes with the activity of SFKs including Lck, as well as other kinases (39). After the deletion of the Lck-binding motif in the CD28 domain of CD28-CAR or CD28-4/1BB-CAR, the CAR-T cells could not produce IL-2 after CAR stimulation and showed improved antitumor performance in the presence of regulatory T cells (40, 41). The CD28-CAR T cells, but not 4/1BB-CAR T cells, resist TGFβ-mediated repression in $TGF\beta^+$ solid tumors (42). However, this resistance is abolished after the deletion of the Lck-binding motif in the CD28 domain in CD28-CAR (42). CAR T cell activation and the Lck-binding motif in CD28 are likely relying mainly on free Lck, as they do not require the canonical pMHC recognition involving coreceptors. Thus, the findings of this research may be applied for designing better immune therapy strategies, especially new CAR-T immunotherapy strategies (43).

Materials and Methods

A detailed description of materials and methods is provided in *SI Appendix, Materials and Methods*. Primary cells were harvested from WT C57BL/6J and OT-I transgenic mice. H2-K^b-OVA APL monomers (NIH Tetramer Core Facility) were tetramerized according to the NIH Tetramer Core Facility protocol. Naïve CD4 T cells ($5–10 \times 10^6$), naïve CD8 T cells, OT-I CTLs, or OT-I hybridoma cells were used for each tetramer stimulation experiment. OT-I hybridoma cells were stimulated with plate-bound antibodies. Ninety-six- or six-well plates were precoated with 1 μg/mL anti-mouse CD3ε and 1 μg/mL anti-CD28 antibodies at 4 °C overnight. FC-IP was done as described previously (22). The Lck sgRNA (sequence: TGTGGTGCAGGAGCGGTGAGTGG) targeting intron and exon junctions was selected based on the off-target and efficiency ranking provided on the CHOPCHOP website (44). FRAP experiments were performed on a Zeiss spinning disk confocal microscope. Images were analyzed using ImageJ (NIH). FRAP measurements were full-scale normalized according to a previously described method (45). The resulting data were fit to a single exponential curve model, and the mobile fraction and half-time recovery was calculated. Mobile fraction is the maximum recovery of fluorescence intensity normalized to the initial fluorescence intensity (as "1") and the fluorescence intensity after photobleaching (as "0").

Data Availability. The sequence of plasmids has been deposited in the National Center for Biotechnology Information GenBank database, https://www.ncbi.nlm.nih.gov/genbank, under accession nos. MT591673–MT591676. All data and associated protocols used for this study are available in the main paper and *SI Appendix*. Cell lines and plasmids used for this study will be available upon request to the corresponding author.

ACKNOWLEDGMENTS. We thank Dr. G. Wright and Dr. W.I. Goh (Institute for Molecular Bioscience [IMB] microscope facility) for helping with the FRAP imaging and Dr. P. Hutchinson and Mr. G. Teo (National University of Singapore Immunology Program Flow Cytometry Laboratory) for helping with the cell sorting. This research was supported by the Singapore Ministry of Health's National Medical Research Council under its CBRG/0097/2015 and by Singapore Ministry of Education's Grant 2014-T2-1-136.

1. N. R. Gascoigne, J. Casas, J. Brzostek, V. Rybakin, Initiation of TCR phosphorylation and signal transduction. *Front. Immunol.* **2**, 72 (2011).
2. E. H. Palacios, A. Weiss, Function of the Src-family kinases, Lck and Fyn, in T-cell development and activation. *Oncogene* **23**, 7990–8000 (2004).
3. M. Reth, Antigen receptor tail clue. *Nature* **338**, 383–384 (1989).
4. H. Wang *et al*., ZAP-70: An essential kinase in T-cell signaling. *Cold Spring Harb. Perspect. Biol.* **2**, a002279 (2010).
5. J. D. Stone, A. S. Chervin, D. M. Kranz, T-cell receptor binding affinities and kinetics: Impact on T-cell activity and specificity. *Immunology* **126**, 165–176 (2009).
6. N. Jiang *et al*., Two-stage cooperative T cell receptor-peptide major histocompatibility complex-CD8 trimolecular interactions amplify antigen discrimination. *Immunity* **34**, 13–23 (2011).
7. T. J. Boggon, M. J. Eck, Structure and regulation of Src family kinases. *Oncogene* **23**, 7918–7927 (2004).
8. P. W. Kim, Z.-Y. J. Sun, S. C. Blacklow, G. Wagner, M. J. Eck, A zinc clasp structure tethers Lck to T cell coreceptors CD4 and CD8. *Science* **301**, 1725–1728 (2003).
9. O. Stepanek *et al*., Coreceptor scanning by the T cell receptor provides a mechanism for T cell tolerance. *Cell* **159**, 333–345 (2014).
10. J. Casas *et al*., Ligand-engaged TCR is triggered by Lck not associated with CD8 coreceptor. *Nat. Commun.* **5**, 5624 (2014).
11. R. J. Salmond, A. Filby, I. Qureshi, S. Caserta, R. Zamoyska, T-cell receptor proximal signaling via the Src-family kinases, Lck and Fyn, influences T-cell activation, differentiation, and tolerance. *Immunol. Rev.* **228**, 9–22 (2009).
12. A. H. Courtney *et al*., A phosphosite within the SH_2 domain of lck regulates its activation by CD_{45}. *Mol. Cell* **67**, 498–511.e6 (2017).
13. L. McNeill *et al*., The differential regulation of Lck kinase phosphorylation sites by CD45 is critical for T cell receptor signaling responses. *Immunity* **27**, 425–437 (2007).
14. G. G. Chiang, B. M. Sefton, Specific dephosphorylation of the Lck tyrosine protein kinase at Tyr-394 by the SHP-1 protein-tyrosine phosphatase. *J. Biol. Chem.* **276**, 23173–23178 (2001).
15. K. Hasegawa *et al*., PEST domain-enriched tyrosine phosphatase (PEP) regulation of effector/memory T cells. *Science* **303**, 685–689 (2004).
16. Y. Arimura, T. Vang, L. Tautz, S. Williams, T. Mustelin, TCR-induced downregulation of protein tyrosine phosphatase PEST augments secondary T cell responses. *Mol. Immunol.* **45**, 3074–3084 (2008).
17. K. Nika *et al*., Constitutively active Lck kinase in T cells drives antigen receptor signal transduction. *Immunity* **32**, 766–777 (2010).
18. P. D. Hsu, E. S. Lander, F. Zhang, Development and applications of CRISPR-Cas9 for genome engineering. *Cell* **157**, 1262–1278 (2014).
19. O. Ballek, J. Valečka, J. Manning, D. Filipp, The pool of preactivated Lck in the initiation of T-cell signaling: A critical re-evaluation of the Lck standby model. *Immunol. Cell Biol.* **93**, 384–395 (2015).
20. K. A. Hogquist *et al*., T cell receptor antagonist peptides induce positive selection. *Cell* **76**, 17–27 (1994).
21. M. A. Daniels *et al*., Thymic selection threshold defined by compartmentalization of Ras/MAPK signalling. *Nature* **444**, 724–729 (2006).
22. A. G. Schrum *et al*., High-sensitivity detection and quantitative analysis of native protein-protein interactions and multiprotein complexes by flow cytometry. *Sci. STKE* **2007**, pl2 (2007). Correction in: *Sci. STKE* **2007**, er3 (2007).
23. A. T. Bida, D. Gil, A. G. Schrum, Multiplex IP-FCM (immunoprecipitation-flow cytometry): Principles and guidelines for assessing physiologic protein-protein interactions in multiprotein complexes. *Methods* **56**, 154–160 (2012).
24. S. E. Smith *et al*., IP-FCM measures physiologic protein-protein interactions modulated by signal transduction and small-molecule drug inhibition. *PLoS One* **7**, e45722 (2012).
25. V. Horkova *et al*., Dynamics of the coreceptor-LCK interactions during T cell development shape the self-reactivity of peripheral CD4 and CD8 T cells. *Cell Rep.* **30**, 1504–1514.e7 (2020).
26. D. L. Wiest *et al*., Regulation of T cell receptor expression in immature CD4+CD8+ thymocytes by p56lck tyrosine kinase: Basis for differential signaling by CD4 and CD8 in immature thymocytes expressing both coreceptor molecules. *J. Exp. Med.* **178**, 1701–1712 (1993).
27. L. Zimmermann *et al*., Direct observation and quantitative analysis of Lck exchange between plasma membrane and cytosol in living T cells. *J. Biol. Chem.* **285**, 6063–6070 (2010).
28. A. M. Akimzhanov, D. Boehning, Rapid and transient palmitoylation of the tyrosine kinase Lck mediates Fas signaling. *Proc. Natl. Acad. Sci. U.S.A.* **112**, 11876–11880 (2015).
29. H. Ike *et al*., Mechanism of Lck recruitment to the T-cell receptor cluster as studied by single-molecule-fluorescence video imaging. *ChemPhysChem* **4**, 620–626 (2003).
30. R. Blanco, A. Borroto, W. Schamel, P. Pereira, B. Alarcon, Conformational changes in the T cell receptor differentially determine T cell subset development in mice. *Sci. Signal.* **7**, ra115 (2014).
31. F. Van Laethem *et al*., Lck availability during thymic selection determines the recognition specificity of the T cell repertoire. *Cell* **154**, 1326–1341 (2013).
32. F. Van Laethem *et al*., Deletion of CD4 and CD8 coreceptors permits generation of alphabetaT cells that recognize antigens independently of the MHC. *Immunity* **27**, 735–750 (2007).
33. R. Bosselut, T. I. Guinter, S. O. Sharrow, A. Singer, Unraveling a revealing paradox: Why major histocompatibility complex I-signaled thymocytes "paradoxically" appear as CD4+8lo transitional cells during positive selection of CD8+ T cells. *J. Exp. Med.* **197**, 1709–1719 (2003).
34. A. Singer, S. Adoro, J. H. Park, Lineage fate and intense debate: Myths, models and mechanisms of CD4- versus CD8-lineage choice. *Nat. Rev. Immunol.* **8**, 788–801 (2008).
35. Y. Cao, J. C. Rathmell, A. N. Macintyre, Metabolic reprogramming towards aerobic glycolysis correlates with greater proliferative ability and resistance to metabolic inhibition in CD8 versus CD4 T cells. *PLoS One* **9**, e104104 (2014).
36. R. J. De Boer, D. Homann, A. S. Perelson, Different dynamics of CD4+ and CD8+ T cell responses during and after acute lymphocytic choriomeningitis virus infection. *J. Immunol.* **171**, 3928–3935 (2003).
37. M. F. Bachmann *et al*., Developmental regulation of Lck targeting to the CD8 coreceptor controls signaling in naive and memory T cells. *J. Exp. Med.* **189**, 1521–1530 (1999).
38. T. L. Geiger, P. Nguyen, D. Leitenberg, R. A. Flavell, Integrated src kinase and costimulatory activity enhances signal transduction through single-chain chimeric receptors in T lymphocytes. *Blood* **98**, 2364–2371 (2001).
39. K. Mestermann *et al*., The tyrosine kinase inhibitor dasatinib acts as a pharmacologic on/off switch for CAR T cells. *Sci. Transl. Med.* **11**, eaau5907 (2019).
40. D. M. Kofler *et al*., CD28 costimulation Impairs the efficacy of a redirected t-cell antitumor attack in the presence of regulatory t cells which can be overcome by preventing Lck activation. *Mol. Ther.* **19**, 760–767 (2011).
41. C. M. Suryadevara *et al*., Preventing lck activation in CAR T cells confers treg resistance but requires 4-1BB signaling for them to persist and treat solid tumors in non-lymphodepleted hosts. *Clin. Cancer Res.* **25**, 358–368 (2019).
42. V. Golumba-Nagy, J. Kuehle, A. A. Hombach, H. Abken, CD28-ζ CAR T cells resist TGF-β repression through IL-2 signaling, which can be mimicked by an engineered IL-7 autocrine loop. *Mol. Ther.* **26**, 2218–2230 (2018).
43. L. Wu, Q. Wei, J. Brzostek, N. R. J. Gascoigne, Signaling from T cell receptors (TCRs) and chimeric antigen receptors (CARs) on T cells. *Cell Mol. Immunol.* **17**, 600–612 (2020).
44. K. Labun, T. G. Montague, J. A. Gagnon, S. B. Thyme, E. Valen, CHOPCHOP v2: A web tool for the next generation of CRISPR genome engineering. *Nucleic Acids Res.* **44**, W272–W276 (2016).
45. N. N. Giakoumakis, M. A. Rapsomaniki, Z. Lygerou, Analysis of protein kinetics using fluorescence recovery after photobleaching (FRAP). *Methods Mol. Biol.* **1563**, 243–267 (2017).